

# Optimal Coordination of Dual-Setting Directional Over Current Relay in Microgrid Considering Multi-Parametric Characteristics

P. Niranjan\*, N.K. Choudhary, N. Singh, R.K. Singh

Department of Electrical Engineering, Motilal National Institute of Technology Allahabad, Prayagraj, India.

**Abstract**— Conventional overcurrent protection schemes may not be sufficient to provide the complete protection of microgrids, especially in the islanded mode (ISM) of operation. Directional overcurrent relays (DOCRs) in microgrid may malfunction due to significant changes in fault current level and change in topology from grid-connected mode (GCM) to ISM. The novel contribution of this study is to determine the optimal settings of time-voltage-current-based dual-setting DOCRs with mixed inverse characteristics, valid in both GCM and ISM, without any miscoordination of relay pairs. The relay coordination problem is formulated as a mixed integer non-linear programming (MINLP) problem and optimally solved using an improved environmental adaption method (IEAM). The proposed relay coordination scheme has been tested on a 7-bus microgrid, the low-voltage section of the modified IEEE-14 bus benchmark system. The performance of the proposed protection scheme has been compared with the existing schemes, considering conventional DOCRs, time-voltage-current-based DOCRs, and dual-setting DOCRs.

**Keywords**—Microgrid, distributed generator, dual-setting DOCRs, protection coordination, IEAM.

## NOMENCLATURE

### Abbreviations

|       |                                                                                        |
|-------|----------------------------------------------------------------------------------------|
| CS    | Relay's curve selection                                                                |
| CTI   | Coordination time interval                                                             |
| DG    | Distributed generator                                                                  |
| DOCRs | Directional overcurrent relays                                                         |
| EI    | Extremely inverse characteristics                                                      |
| FL    | Fault location                                                                         |
| GA    | Genetic algorithm                                                                      |
| GCM   | Grid-connected mode                                                                    |
| IEAM  | Improved environmental adaption method                                                 |
| IIDG  | Inverter interfaced DG                                                                 |
| ISM   | Islanded mode                                                                          |
| LCT   | Least coordination time                                                                |
| LP    | Linear programming                                                                     |
| MI    | Mixed inverse characteristics                                                          |
| MINLP | Mixed-integer nonlinear programming problem                                            |
| NLP   | Nonlinear programming                                                                  |
| OBJ   | The objective function which represents the total operating time of dual-setting DOCRs |
| PS    | Plug setting                                                                           |
| PSO   | Particle swarm optimization                                                            |
| RMDG  | Rotating machine-based DG                                                              |
| SI    | Standard inverse characteristics                                                       |
| TMS   | Time multiplier setting                                                                |
| VI    | Very inverse characteristics                                                           |

## 1. INTRODUCTION

The protection of microgrids is a significant challenge as the fault current magnitude varies significantly depending on its mode

of operation. The fault current also depends upon the distributed generator (DG) type, namely, inverter interfaced DG (IIDG) and conventional rotating machine-based DG (RMDG) [1–3]. Integration of DG may cause several challenges in microgrids, such as; false tripping, blinding of protection, etc., making it difficult to protect the microgrids [4, 5]. As a result, current research is focused on improving protection schemes to mitigate the impact of DG integration on protection coordination.

DOCRs are one of the most efficient and economical devices to protect the microgrid from overcurrent. The optimal settings and characteristic curves of the DOCRs can be obtained to achieve proper coordination [6, 7]. Several protection strategies incorporating conventional DOCRs [8, 9], time-voltage-current-based DOCRs [10], dual-setting DOCRs [11], and time-voltage-current-based dual-setting DOCRs with standard characteristics have been proposed to solve the relay coordination problem [12]. Conventional and time-voltage-current-based DOCRs are associated with a single relay setting for primary and backup protection. However, dual-setting and time-voltage-current-based dual-setting DOCRs are associated with two different settings, depending upon the direction of the short circuit current. The same relay acts as a primary protective device for the forward direction of the fault current and as a backup protective device for the reverse direction of the fault current.

According to the IEC-60255 standard, conventional DOCRs operating time is determined by their time-current characteristics, which are categorized as standard inverse (SI), very inverse (VI), and extremely inverse (EI) [6]. Usually, the SI characteristic of DOCRs is considered to protect the microgrid in the GCM. However, DOCRs with SI characteristics in the ISM may take more time to sense the fault [13]. As a result, the microgrid will be stressed for longer period during faults, potentially causing damage to the entire system. Therefore, along with SI characteristics, EI and VI characteristics of DOCRs are better suited to protect microgrids. Thus, the optimal selection of these characteristics makes the relay coordination scheme more flexible, termed the relay's curve selection (CS). Therefore, along with the time multiplier setting (TMS) and plug setting (PS), a third variable, CS, is also considered for each DOCR [6, 14].

Received: 17 Apr. 2023

Revised: 17 Jul. 2023

Accepted: 18 Aug. 2023

\*Corresponding author:

E-mail: priyanshul.2018ree04@mnnit.ac.in (P. Niranjan)

DOI: 10.22098/JOAPE.2023.12725.1965

Research Paper

© 2023 University of Mohaghegh Ardabili. All rights reserved

Depending on the variables, the relay coordination problem can be expressed as linear programming (LP), nonlinear programming (NLP), and MINLP. In LP, only TMS is used as a decision variable, while PS remains constant, whereas, in NLP, both are treated as continuous decision variables. In MINLP, TMS and PS are considered continuous and discrete variables. With the above schemes, the optimal PS and TMS values are determined by using an improved firefly algorithm [15], revised simplex method [16, 17], genetic algorithm (GA) [18], modified firefly algorithm [19], gravitational search algorithm [20], differential evolution [21], GA-LP [22], fuzzy-based GA [23] and multi-objective PSO [24], etc.

To overcome the maloperation of DOCRs in the microgrid, several protection schemes are proposed that are valid in either of the operating modes, i.e., DOCRs have two different settings, one for each operating mode. The main disadvantage of different settings is that the optimal settings of DOCRs obtained for ISM can cause miscoordination of relay pairs in the GCM and vice versa [8]. To provide the best protection coordination valid in both operating modes, the common optimal settings of DOCRs must be obtained. The optimal solution to the relay coordination problem is obtained using IEAM and compared to existing schemes in the literature. The evaluation includes the total operating time of DOCRs, fault discrimination capability, and coordination accuracy. The test system is simulated in the MATLAB/SIMULINK 2018a at 2.5 GHz on a Core i5-7200U processor. The complete steps of the proposed protection coordination scheme is shown in Fig. 1. The significant contributions of the study are as below:

- A modified protection coordination scheme is proposed to determine the common optimal settings of user-defined time-voltage-current-based dual-setting DOCRs considering MI characteristics.
- To determine common optimal settings of time-voltage-current-based dual-setting DOCRs, valid in both the operating modes of the microgrid without any miscoordination of relay pairs.
- The optimal solution to the relay coordination problem is obtained using IEAM.
- Compared to existing schemes, the proposed relay coordination scheme significantly reduces the total operating time of DOCRs.

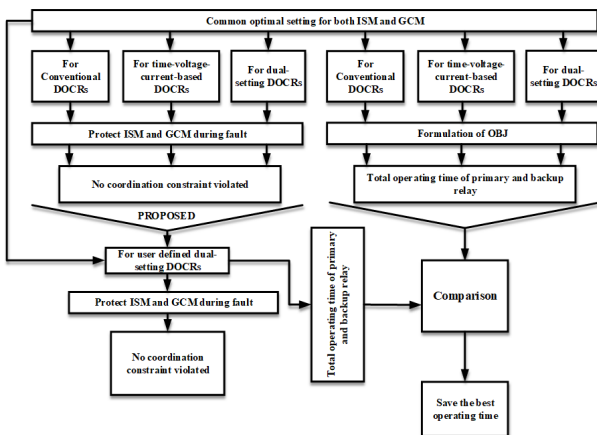


Fig. 1. Proposed common optimal settings of time-voltage-current-based dual-setting DOCRs for both ISM and GCM.

The rest of the paper is structured as follows. Section 2 explains the relay coordination problem formulation considering all the protection strategies and details of IEAM. Section 3 briefly discusses the test system, while Section 4 presents the results and discussion. The conclusion and future direction of the study are included in section 5.

Table 1. DOCR characteristic curve coefficients (IEC-60255 std.).

| Relay Characteristics | $A_D$ | $B_D$ | CS |
|-----------------------|-------|-------|----|
| SI                    | 0.14  | 0.02  | 3  |
| EI                    | 80    | 2     | 2  |
| VI                    | 13.5  | 1     | 1  |

## 2. RELAY COORDINATION PROBLEM FORMULATION

The relay coordination problem formulation has been divided into two sections: one for formulating the objective function and constraints and the other for obtaining the optimal solution.

### 2.1. Relay characteristics

Depending on the manufacturer, the characteristic equation controlling the operating time of DOCRs varies. Conventional DOCRs with time-current characteristics are characterized by the IEC-60255 standard, as shown by Eq. (1) [8], where  $A_D$  and  $B_D$  vary with the relay characteristic types, as mentioned in Table 1.

$$t_{p,i} = A_D \frac{TMS_i}{\left(\frac{I_{sc,i}}{CT_{Ratio,i} \times PS_i}\right)^{B_D} - 1} \quad (1)$$

In Eq. (1),  $t_{p,i}$  represents the operating time of the  $i_{th}$  relay. Whereas,  $I_{sc,i}$ ,  $CT_{Ratio,i}$ ,  $PS_i$ , and  $TMS_i$  are the fault current, current transformer ratio, plug setting, and time multiplier setting, respectively of the  $i_{th}$  relay. The overcurrent protection alone may be ineffective in detecting the faults in the ISM of microgrid especially with IIDGs as the generating units. As voltage drop occurs during the fault; therefore, the time-voltage-current-based relay characteristic can be a viable solution to the relay coordination problem, especially in ISM of the microgrid. In [12], a DOCR with a time-voltage-current-based characteristic is proposed. DOCRs with such characteristic isolate the fault in lesser time than the conventional DOCRs with time-current characteristics. The operating time of DOCRs having time-voltage-current-based characteristics is represented by Eq. (2). In Eq. (2), the per-unit phase voltage for the  $i_{th}$  relay is denoted as  $v_{f_i}$  and  $\alpha$  is considered as a decision variable.

$$t_{p,i} = A_D \frac{TMS_i}{\left(\frac{I_{sc,i}}{CT_{Ratio,i} \times PS_i}\right)^{B_D} - 1} \times \left(\frac{1}{e^{1-v_{f_i}}}\right)^\alpha \quad (2)$$

In contrast, dual-setting DOCRs with two sets of optimal settings have been proposed in [11]. The proposed protection coordination scheme combines the time-voltage-current characteristics with the dual-setting feature to propose a time-voltage-current-based dual-setting DOCR. The relay consists of two distinct pairs of settings,  $(TMS_{fw}, PS_{fw})$  and  $(TMS_{rv}, PS_{rv})$  for the forward and reverse direction of fault currents, respectively. The operating time of time-voltage-current-based dual-setting DOCR for forward and reverse the direction of fault currents are shown in Eq. (3) and Eq. (4), respectively.

$$t_{fw,i}^p = A_D \frac{TMS_{fw,i}}{\left(\frac{I_{sc,i}}{CT_{Ratio,i} \times PS_{fw,i}}\right)^{B_D} - 1} \times \left(\frac{1}{e^{1-v_{f_i}}}\right)^\alpha \quad (3)$$

$$t_{rv,k}^b = A_D \frac{TMS_{rv,k}}{\left(\frac{I_{sc,k}}{CT_{Ratio,k} \times PS_{rv,k}}\right)^{B_D} - 1} \times \left(\frac{1}{e^{1-v_{f_k}}}\right)^\alpha \quad (4)$$

$$OBJ = \min_{TMS_{fw}, PS_{fw}, TMS_{rv}, PS_{rv}} \sum_{i=1}^n \sum_{j=1}^m \left( t_{fw,i,j}^p + \sum_{k=1}^K t_{rv,k,j}^b \right) \quad (5)$$

In Eqs. (3) and (4),  $t_{fw,i}^p$  and  $t_{rv,k}^{bk}$  are the operating time of  $i_{th}$  primary and corresponding  $k_{th}$  backup relays for forward and reverse the direction of fault currents, respectively. The protection coordination scheme aims to minimize the total operating time of primary and backup relays subjected to coordination constraints validation. The objective function (OBJ) representing the overall relay operating time is expressed by Eq. (5). All the constraints must be satisfied to achieve the best feasible solution for each relay. The constraints of the proposed relay coordination scheme are expressed from Eqs. (6)-(11). The minimum and maximum limits of TMS for the forward and reverse direction of fault currents are considered 0.1s and 1.1s, respectively [6]. The PS lies between 0.5 and 2.0 [6]. The operating time range of each dual-setting DOCR for the forward ( $t_{fw,i}^p$ ) and reverse direction ( $t_{rv,k}^{bk}$ ) is considered from 0.1 – 4.0s, and the value of  $\alpha$  lies between 0-5 [6, 10]. The difference between the operation of the primary and backup relay is termed as least coordination time (LCT), which is considered 0.2s in this study.

$$TMS_{min,i} \leq TMS_{fwi}, TMS_{rvk} \leq TMS_{max,k} \quad (6)$$

$$PS_{min,i} \leq PS_{fwi}, PS_{rvk} \leq PS_{max,k} \quad (7)$$

$$t_{min,i}^p \leq t_{fw,i}^p \leq t_{max,i}^p \quad (8)$$

$$t_{min,k}^b \leq t_{rv,k}^{bk} \leq t_{max,k}^b \quad (9)$$

$$0 \leq \alpha \leq 5 \quad (10)$$

$$t_{rv,k}^{bk} - t_{fw,i}^p \geq LCT \quad (11)$$

In the above-mentioned Equations,  $i$  represents the index of the primary relay, which ranges from 1 to  $n$ , where  $n$  is the total number of primary relays in the system. Index  $k$  represents the corresponding backup relay associated with the primary relay. It ranges from 1 to  $K$ , where  $K$  is the system's total number of corresponding backup relays. Index  $j$  represents the fault location, which ranges from 1 to  $m$ , where  $m$  is the total number of fault locations considered.

## 2.2. Improved environment adaptation method (IEAM)

The optimization algorithm minimizes searching time to reach the optimal global solution. IEAM is an improved version of the environment adaptation method [25]. The IEAM utilizes the concepts of particle swarm optimization (PSO) so that the regions discovered by the operators of the environment adaptation method can be exploited [25, 26].

This algorithm uses three different operators, namely the adaption operator, alteration operator, and selection operator. The adaptation operator update the solution  $P_i$  as given in Eq. (12).  $F(P_i)$  is the fitness value of  $P_i$ , and  $\alpha, \beta$  represents the random values to be determined based on the requirements. The total number of bits for an individual is represented by  $l$  and  $F_{avg}$  represents the current population's average fitness value. A new solution  $P_{i+1}$  is generated by alteration operator by flipping one or more bits of  $P_i$ . The function of the selection operator is to select the best solutions equal to the size of the initial population.

$$P_{i+1} = (\alpha * (P_i)^{F(P_i)/F_{avg}} + \beta)/(2^l - 1) \quad (12)$$

In Eq. (12),  $i$  represents the index of individual in binary,  $P$  represents the temporary pool and  $\alpha, \beta$  represents the random numbers. The adaptation operator is slightly changed compared to the primary or classical environment adaptation method algorithm. In environment adaptation method, the structure of the particle is updated based on the change in an environment only, and there is no role of the best particle in it. However, in the PSO algorithm, the particle's genetic structure also helps to find the best solution. The same idea is used in IEAM, in which the solution structure is upgraded using the guidelines from the genomic structure of the optimal solutions from both the previous and current generations.

The idea that the best solution will use the adaption operator of environment adaptation method and explore the entire search space prevents the problem of stagnation, as in PSO. The operator shown in Eq. (13) is used by all solutions besides the best solution in IEAM.

$$P_{i+1} = (\alpha * (\text{Decoded value in decimal of binary version of } P_{in})F(X_i)/F_{avg} + \beta\{(G_i - P_i)\})/(2^l) \quad (13)$$

Where  $G_i$  is the best particle's vector position, and  $P_i$  is the position value of the particle that is supposed to update its structure. The adaptation operator is used to achieve the best solution, as shown by Eq. (14).

$$P_{i+1} = (\alpha * (\text{Decoded value in decimal of binary version of } P_{in})F(X_i)/F_{avg} + \beta)/(2^l) \quad (14)$$

The parameter values  $\alpha$  and  $\beta$  are chosen in IEAM such that in the early generation the global optimal global solution can be determined. For the optimal solution, the value of  $\alpha$  is considered as  $(2^l)$ , and  $\beta$  is set to 0.5. To terminate the algorithm, the ratio of  $F_{avg}$  and  $F(G_i)$  is checked in each generation, which provides information about the solution's clustering. When all solutions converge on one point, the ratio becomes one. If the value of  $F_{avg}/F(G_i)$  is greater than or equal to 0.8, the algorithm is converges to provide the global optimum solutions. In this case,  $\alpha$  is set to be very high to perturb the current generation's solutions and avoid premature convergence. The value of  $\alpha$  is stretched again and again until a stable solution is obtained.

## 2.3. Protection coordination methodologies for optimal settings of DOCRs

The optimal settings of DOCRs obtained for ISM may miscoordinate the relay pairs in the GCM and vice-versa. This necessitates the calculation of common optimal settings of DOCRs, suitable to provide optimal protection coordination in both operating modes. The effects of GCM and ISM are combined to obtain the common optimal settings of DOCRs. As a result, the total number of primary and corresponding backup relay pairs doubles. As the constraints of both operating modes are considered together, coordination can be maintained in both modes of microgrid with the settings obtained.

To achieve proper coordination among DOCRs, optimal selection of relay parameters, i.e., TMS, PS, and  $\alpha$ , is one of the most essential requirements. In this context, the selection of optimization technique is crucial from the points of lesser reaction time, convergence time, global optimal solutions, etc. Considering all these aspects, three algorithms, namely IEAM, PSO, and GA, are used as optimization tools to determine the optimal solution of the protection coordination problem. These algorithms have been executed several times with different sets of parameters to obtain the minimum total operating time of primary relays with lesser iterations, as shown in Table 2.

Each algorithm has been executed 50 times to evaluate the reproducibility of the results obtained. Subsequently, with these results, various statistical parameters, such as best time, worst time, etc., have been calculated for overall comparison. Fig. 2

Table 2. Algorithm parameters.

| Optimization technique | Parameters               |
|------------------------|--------------------------|
| IEAM                   | Iteration: 200           |
|                        | Population size: 50      |
|                        | Alpha: 0.2               |
|                        | Beta: 0.5                |
| PSO                    | $F_{avg}/F(G_i)$ :0.8    |
|                        | Iteration: 200           |
|                        | Population size: 50      |
|                        | Inertia Weight: 0.9      |
| GA                     | Cognitive Coefficient: 1 |
|                        | Maximum Velocity: 5      |
|                        | Iteration: 200           |
|                        | Population size: 50      |

shows the flowchart of the overall procedure to achieve the best optimal solution. The common optimal settings of DOCRs have been determined with the following steps shown in Fig. 3.

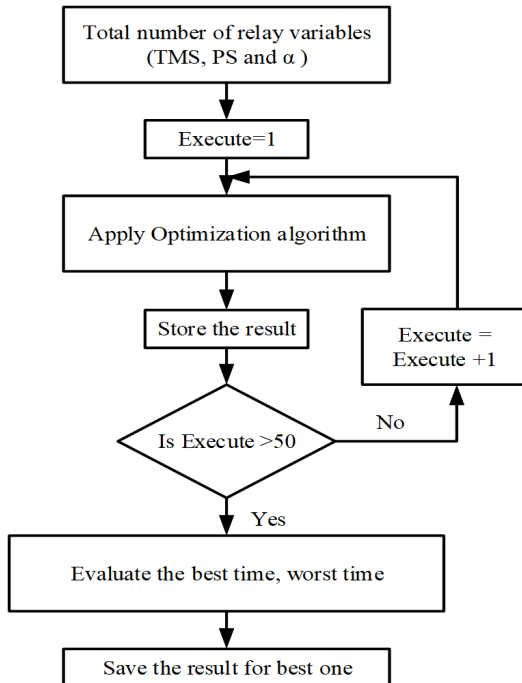


Fig. 2. Procedure to obtain the best optimal settings.

### 3. TEST SYSTEM AND SIMULATION

The performance of the proposed relay coordination scheme has been tested on the IEEE-14 bus benchmark system's low voltage (11kV) section, as shown in Fig. 4 [27]. It consists of two 20 MVA IIDGs connected at buses B2 and B7 and a 50 MVA conventional rotating machine-based DG connected at bus B1. In GCM, the 7-bus microgrid has the highest generation capacity of 60 MVA linked to the sub-transmission system through buses B3 and B6. The maximum short-circuit levels of the generators are 250 MVA, 80 MVA, 300 MVA, 300 MVA, and 80 MVA connected at B1, B2, B3, B6, and B7, respectively.

In the test system, three-phase midpoint faults have been created at different fault locations (L1- L8). Based upon these fault locations, the 22 relay pairs (primary and backup relays) have been identified, for each operating mode. The system is equipped with 16 DOCRs (R1 to R16), providing complete protection to the 7-bus microgrid. Relay pairs are formed by considering different fault locations. For example, R1 and R2 (forward operation) are the primary relays for fault at L1. The backup relays for RL1 are

R3 and R5 (reverse operation), whereas R7 (reverse operation) is the backup relay for R2. The fault currents and voltages in both operating modes of the microgrid, along with the details of 22 primary backup relay pairs, are shown in Table 3. The  $CT_{Ratio,i}$  for the relays are found using Eq. (15), where,  $I_{f\max,i}$  and  $I_{L\max,i}$  are the maximum short circuit current and maximum load current for the  $i_{th}$  relay, respectively, as shown in Table 4 [6].

$$CT_{Ratio,i} = \text{Maximum} \left( I_{L\max,i}, \frac{I_{f\max,i}}{20} \right) \quad (15)$$

## 4. RESULTS AND DISCUSSION

The performance of dual-setting DOCRs coordination with MI characteristics has been tested in GCM and ISM. Further, common optimal settings of dual-setting DOCRs have been determined to remain valid in both operating modes, simultaneously. The results of the proposed coordination scheme have been compared with the existing techniques, namely, conventional DOCRs, time-voltage-current-based DOCRs, and dual-setting DOCRs.

### 4.1. Optimal coordination of conventional DOCRs, time-voltage-current-based DOCRs, and dual-setting DOCRs

The optimal protection coordination study of conventional DOCRs, DOCRs with time-voltage-current-based characteristics, and dual-setting DOCRs has been presented in this section. The performance of the protection scheme has been accessed by determining the common optimal setting of relays, valid for both GCM and ISM of the 7-bus microgrid.

Table 5 shows the optimal relay settings and total operating time of the conventional DOCRs, time-voltage-current-based DOCRs, and dual-setting DOCRs with MI characteristics, i.e., the combination of the SI, VI, and EI characteristics. For conventional DOCRs, time-voltage-current-based DOCRs, and dual-setting DOCRs, the total operating time of relays with common optimal settings are 15.1320s, 13.7985s, and 11.4531s, respectively. For time-voltage-current-based DOCRs,  $\alpha$  is an optimally determined variable, as shown in Table 4. The least total operating time of relays is obtained using dual-setting DOCRs. The operating time of primary and corresponding backup relay pairs and the actual LCT for conventional DOCRs, DOCRs with time-voltage-current-based characteristics, and dual-setting DOCRs with the common optimal settings are shown in Figs. 5, 6, and 7, respectively. The first pairs of 22 relays and the remaining 22 relay pairs correspond to the GCM and ISM.

Furthermore, it is found that LCT is always greater than the fixed CTI. It is observed that the performance of the coordination scheme is best for dual-setting DOCRs as the total operating time of relays is the least. It indicates that the best solution can be obtained if the time-voltage-current characteristics are combined with the features of dual-setting DOCRs. Therefore, the protection coordination study of time-voltage-current-based dual-setting DOCRs is discussed in Section 4.2.

### 4.2. Protection scheme with time-voltage-current-based dual-setting DOCRs

The upgraded time-voltage-current-based dual-setting DOCR can operate for both forward and reverse directions of fault currents. The optimal relay settings and total operating time of the modified dual-setting DOCRs with the MI characteristics for ISM and GCM are shown in Tables 6 and 7, respectively. However, the common optimal settings of the relays valid for either of the operating modes are shown in Table 8. The optimal values of  $\alpha$  obtained in different modes are shown in Tables 6, 7, and 8, respectively.

Fig. 8 depicts the operating time of primary-backup relay pairs and actual LCT in ISM and GCM. Whereas, with the common



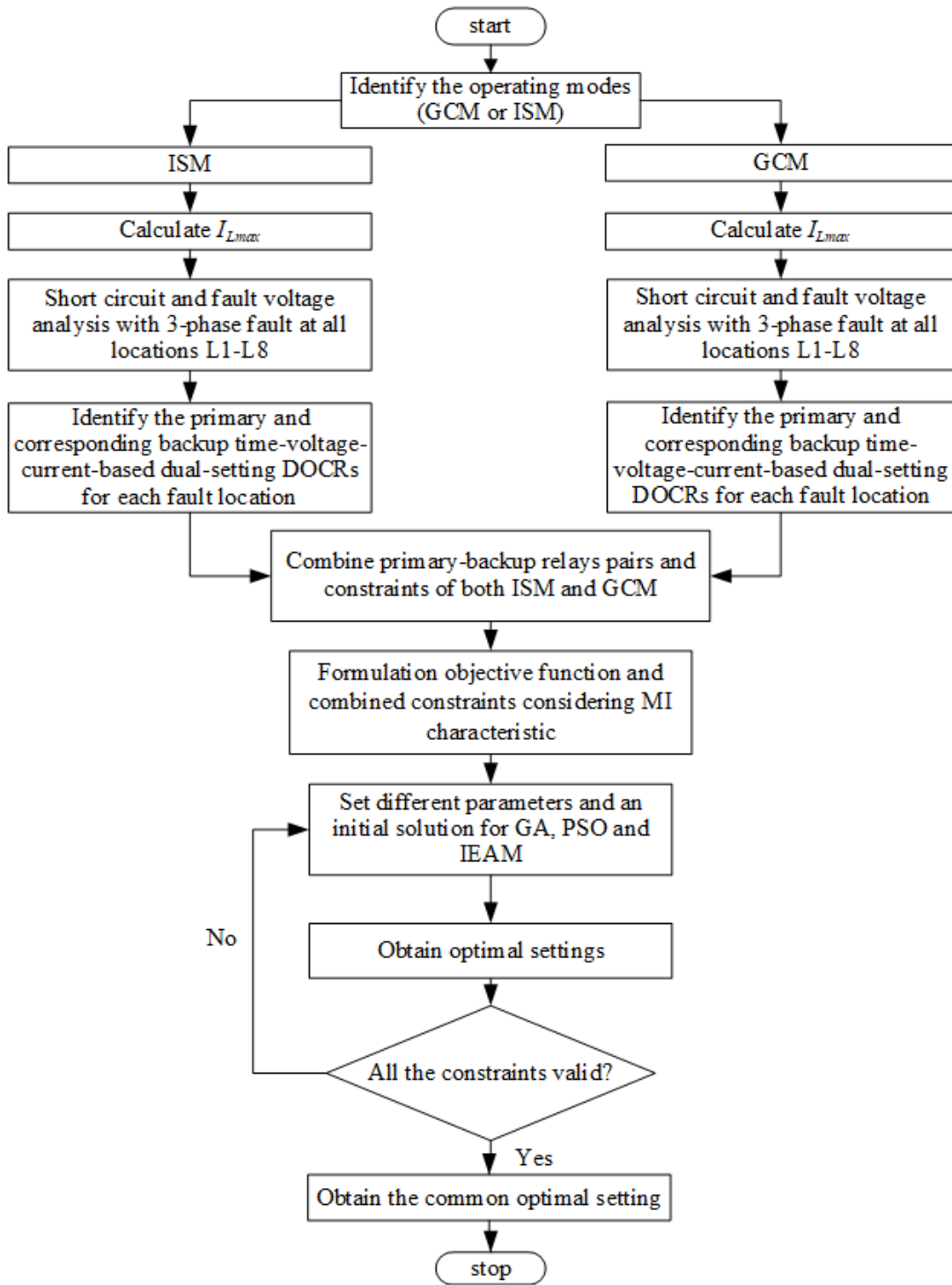


Fig. 3. Proposed coordination scheme for common optimal settings of time-voltage-current-based dual-setting DOCRs.

optimal settings, the operating time and LCT of the relay pairs are shown in Fig. 9. The operating time of DOCRs and LCTs of primary and corresponding backup relay pairs with common relay settings are less than that of individual ISM and GCM. Also, the LCT is always more than the fixed CTI. Thus, the least operating time is obtained with the common optimal settings for the proposed time-voltage-current based dual-setting DOCRs.

#### 4.3. Coordination constraint violations and comparison of the results obtained

The number of coordination constraint violations in all operating modes of the microgrid with MI characteristics are shown in Table 9. For each protection scheme, several constraints violations occur when the optimal settings for the GCM are applied to the ISM and vice-versa. Furthermore, with the obtained common optimal settings, no constraints are violated in either of the operating modes. Therefore, the obtained common settings are the best solution to the relay coordination problem in microgrids.

Table 3. Currents and voltages in GCM and ISM for primary (P) and backup relay (B) pairs.

| FL | S. N. | P   | B (dual) | GCM             |                 | ISM             |                 | ISM           |               | GCM           |               |
|----|-------|-----|----------|-----------------|-----------------|-----------------|-----------------|---------------|---------------|---------------|---------------|
|    |       |     |          | Currents        |                 |                 |                 | Voltages      |               |               |               |
|    |       |     |          | $I_{fprim}$ (A) | $I_{fback}$ (A) | $I_{fprim}$ (A) | $I_{fback}$ (A) | $V_{rv}$ (pu) | $V_{fw}$ (pu) | $V_{fw}$ (pu) | $V_{rv}$ (pu) |
| L1 | 1     | R1  | R3       | 4830            | 1914            | 3612            | 384             | 0.1334        | 0.1334        | 0.1784        | 0.1784        |
|    | 2     | R1  | R5       | 4830            | 812             | 3612            | 564             | 0.1334        | 0.1334        | 0.1784        | 0.1784        |
|    | 3     | R2  | R7       | 3435            | 2069            | 2305            | 726             | 0.0851        | 0.0851        | 0.1269        | 0.1269        |
| L2 | 4     | R3  | R1       | 5737            | 1641            | 4844            | 959             | 0.0674        | 0.0674        | 0.0798        | 0.0798        |
|    | 5     | R3  | R5       | 5737            | 694             | 4844            | 333             | 0.0674        | 0.0674        | 0.0798        | 0.0798        |
|    | 6     | R4  | R14      | 6430            | 1587            | 2140            | 954             | 0.0298        | 0.0298        | 0.0895        | 0.0895        |
|    | 7     | R4  | R15      | 6430            | 543             | 2140            | 1057            | 0.0298        | 0.0298        | 0.0895        | 0.0895        |
| L3 | 8     | R5  | R1       | 5503            | 1308            | 3968            | 928             | 0.1126        | 0.1126        | 0.1562        | 0.1562        |
|    | 9     | R5  | R3       | 5503            | 1600            | 3968            | 323             | 0.1126        | 0.1126        | 0.1562        | 0.1562        |
|    | 10    | R6  | R16      | 3357            | 1980            | 2345            | 835             | 0.0665        | 0.0665        | 0.0953        | 0.0953        |
| L4 | 11    | R7  | R2       | 3519            | 1988            | 3087            | 1469            | 0.0879        | 0.0879        | 0.1002        | 0.1002        |
|    | 12    | R8  | R9       | 5374            | 1170            | 1963            | 1403            | 0.0559        | 0.0559        | 0.1530        | 0.1530        |
| L5 | 13    | R9  | R8       | 8019            | 1948            | 2678            | 2087            | 0.0230        | 0.0230        | 0.0690        | 0.0690        |
|    | 14    | R10 | R11      | 2792            | 2607            | 2076            | 1886            | 0.0179        | 0.0179        | 0.0240        | 0.0240        |
| L6 | 15    | R11 | R10      | 4777            | 4648            | 2197            | 2008            | 0.0437        | 0.0437        | 0.0951        | 0.0951        |
|    | 16    | R12 | R13      | 3590            | 3544            | 2470            | 2419            | 0.0492        | 0.0492        | 0.0714        | 0.0714        |
| L7 | 17    | R13 | R12      | 2926            | 2879            | 1548            | 1486            | 0.0325        | 0.0325        | 0.0614        | 0.0614        |
|    | 18    | R14 | R4       | 6626            | 2206            | 3862            | 2548            | 0.0811        | 0.0811        | 0.1391        | 0.1391        |
|    | 19    | R14 | R15      | 6626            | 964             | 3862            | 1173            | 0.0811        | 0.0811        | 0.1391        | 0.1391        |
| L8 | 20    | R15 | R4       | 5673            | 1219            | 3048            | 2091            | 0.0824        | 0.0824        | 0.1534        | 0.1534        |
|    | 21    | R15 | R14      | 5673            | 1245            | 3048            | 2091            | 0.0824        | 0.0824        | 0.1534        | 0.1534        |
|    | 22    | R16 | R6       | 3115            | 1829            | 2606            | 1233            | 0.0705        | 0.0705        | 0.0842        | 0.0842        |

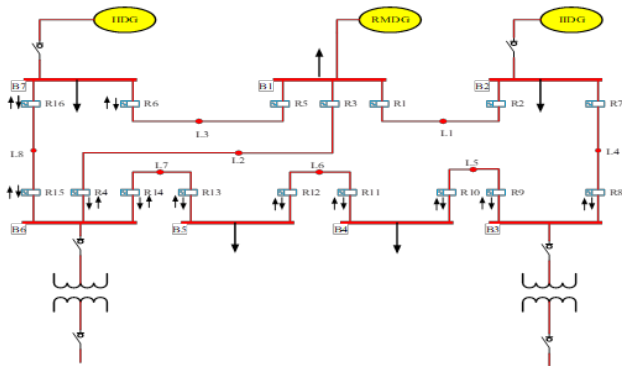


Fig. 4. The 7-bus microgrid (low voltage part of the IEEE-14 bus system).

Table 4. CTR of each dual-setting DOCRs.

| DOCR | Conventional DOCRs |                       | dual-setting DOCRs    |                      |
|------|--------------------|-----------------------|-----------------------|----------------------|
|      | CTR for each relay | CTR for primary relay | CTR for primary relay | CTR for backup relay |
| R1   | 2000/5             | 2000/5                | 2000/5                | 1000/5               |
| R2   | 1000/5             | 1000/5                | 2000/5                | 2000/5               |
| R3   | 3000/5             | 3000/5                | 3000/5                | 2000/5               |
| R4   | 2000/5             | 2000/5                | 3000/5                | 3000/5               |
| R5   | 1600/5             | 1600/5                | 1600/5                | 1000/5               |
| R6   | 1000/5             | 1000/5                | 1000/5                | 1600/5               |
| R7   | 2500/5             | 2500/5                | 2500/5                | 1600/5               |
| R8   | 1600/5             | 1600/5                | 2500/5                | 2500/5               |
| R9   | 2500/5             | 2500/5                | 1200/5                | 1200/5               |
| R10  | 1200/5             | 1200/5                | 2500/5                | 2500/5               |
| R11  | 1200/5             | 1200/5                | 2500/5                | 2500/5               |
| R12  | 2500/5             | 2500/5                | 1200/5                | 1200/5               |
| R13  | 800/5              | 800/5                 | 3000/5                | 3000/5               |
| R14  | 3000/5             | 3000/5                | 800/5                 | 800/5                |
| R15  | 1600/5             | 1600/5                | 1600/5                | 1600/5               |
| R16  | 1600/5             | 1600/5                | 1600/5                | 1600/5               |

Table 10 compares the total operating time of DOCRs for all the protection schemes in the GCM, ISM, and common operating modes (for GCM and ISM) of the microgrid. The total operating time in both modes is significantly less for the proposed time-voltage-current-based dual-setting DOCRs. The total relay operating times are reduced by 27.69%, 20.66%, and 10.40% in common mode compared to conventional DOCRs, time current-based DOCRs, and dual-setting DOCRs, respectively. To

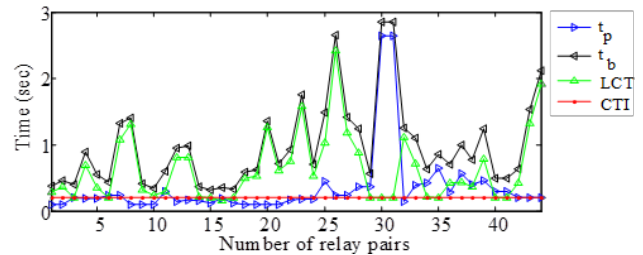


Fig. 5. Operating time and LCT of conventional DOCRs for common optimal settings using IEAM.

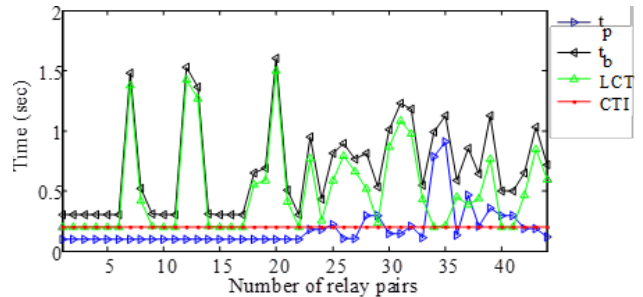


Fig. 6. Operating time and LCT of time-voltage-current-based DOCRs for common optimal settings using IEAM.

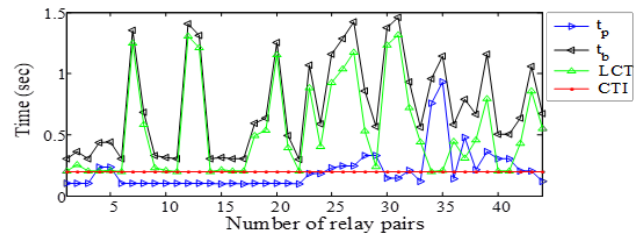


Fig. 7. Operating time and LCT of dual-setting DOCRs for common optimal settings using IEAM.

validate the effectiveness of the proposed scheme, the IEAM

Table 5. Common optimal settings of DOCRs with MI characteristics using IEAM algorithm.

| Relay      | Conventional DOCRs |        | Time-voltage-current-based DOCRs |        |          | Dual-setting DOCRs |               |                |               | CS |
|------------|--------------------|--------|----------------------------------|--------|----------|--------------------|---------------|----------------|---------------|----|
|            | TMS (s)            | PS (A) | TMS (s)                          | PS (A) | $\alpha$ | $TMS_{FW}$ (s)     | $PS_{FW}$ (A) | $TMS_{RV}$ (s) | $PS_{RV}$ (A) |    |
| R1         | 0.592              | 0.553  | 0.104                            | 1.427  | 0.209    | 0.210              | 0.938         | 0.841          | 0.656         | 2  |
| R2         | 0.986              | 0.866  | 0.291                            | 1.500  | 0.296    | 0.453              | 0.916         | 0.336          | 0.524         | 2  |
| R3         | 0.168              | 0.762  | 0.162                            | 0.773  | 0.026    | 0.101              | 0.500         | 0.100          | 0.500         | 3  |
| R4         | 0.115              | 0.609  | 0.161                            | 0.597  | 0.639    | 0.236              | 0.500         | 0.255          | 0.541         | 1  |
| R5         | 0.388              | 0.974  | 0.647                            | 1.297  | 1.287    | 0.253              | 0.500         | 0.100          | 0.854         | 1  |
| R6         | 0.236              | 0.512  | 0.139                            | 1.023  | 0.220    | 0.546              | 0.810         | 0.255          | 0.688         | 2  |
| R7         | 0.737              | 0.500  | 0.100                            | 1.494  | 0.558    | 0.100              | 0.500         | 0.166          | 0.770         | 1  |
| R8         | 0.240              | 0.710  | 0.160                            | 1.441  | 0.800    | 1.089              | 0.570         | 0.829          | 0.543         | 2  |
| R9         | 0.124              | 1.500  | 0.535                            | 0.546  | 0.464    | 0.647              | 0.712         | 0.263          | 1.220         | 2  |
| R10        | 0.116              | 1.484  | 1.080                            | 0.516  | 0.306    | 0.162              | 0.514         | 0.410          | 0.500         | 1  |
| R11        | 1.020              | 0.759  | 1.092                            | 0.921  | 0.621    | 0.826              | 0.774         | 0.354          | 0.534         | 2  |
| R12        | 0.432              | 0.532  | 0.188                            | 0.774  | 0.042    | 0.236              | 0.524         | 0.709          | 0.875         | 2  |
| R13        | 0.428              | 1.114  | 0.944                            | 0.771  | 0.207    | 0.446              | 0.966         | 0.142          | 0.949         | 2  |
| R14        | 0.239              | 0.796  | 0.277                            | 1.524  | 1.697    | 0.365              | 0.651         | 0.290          | 1.124         | 2  |
| R15        | 0.100              | 1.259  | 0.329                            | 0.934  | 1.068    | 0.100              | 1.238         | 0.222          | 0.526         | 1  |
| R16        | 0.234              | 0.500  | 0.138                            | 0.895  | 0.277    | 0.135              | 0.505         | 0.156          | 0.797         | 1  |
| <b>OBJ</b> | <b>15.1320s</b>    |        | <b>13.7985s</b>                  |        |          | <b>11.4531s</b>    |               |                |               |    |

Table 6. Optimal settings of time-voltage-current-based dual-setting DOCRs in ISM using IEAM.

| Relay      | $TMS_{FW}$ (s)   | $PS_{FW}$ (A) | $\alpha$ | $TMS_{RV}$ (s) | $PS_{RV}$ (A) | $\alpha$ | CS |  |
|------------|------------------|---------------|----------|----------------|---------------|----------|----|--|
| R1         | 0.3500           | 0.5866        | 0.0352   | 0.1000         | 0.5324        | 0.0144   | 2  |  |
| R2         | 0.8417           | 0.9551        | 1.3062   | 0.1000         | 0.5000        | 0.2969   | 2  |  |
| R3         | 0.9670           | 0.5000        | 0.2022   | 0.9081         | 0.5000        | 1.2930   | 1  |  |
| R4         | 0.1340           | 0.5145        | 0.0005   | 0.1000         | 0.8651        | 0.0613   | 2  |  |
| R5         | 0.1607           | 0.5467        | 0.0001   | 0.3034         | 0.5000        | 1.8138   | 2  |  |
| R6         | 0.9244           | 0.5170        | 0.3907   | 0.9440         | 1.8125        | 1.0820   | 1  |  |
| R7         | 0.1000           | 0.8835        | 0.2644   | 1.1000         | 0.8856        | 2.1199   | 2  |  |
| R8         | 1.1000           | 0.5000        | 1.3671   | 0.6410         | 0.5106        | 1.3727   | 2  |  |
| R9         | 0.1343           | 0.5145        | 0.0001   | 0.5335         | 0.5000        | 0.2500   | 2  |  |
| R10        | 0.3500           | 0.7629        | 0.2557   | 0.4854         | 0.5000        | 0.3280   | 2  |  |
| R11        | 0.9750           | 1.2823        | 2.3943   | 0.5078         | 0.5000        | 0.1232   | 2  |  |
| R12        | 0.2054           | 0.5815        | 0.7588   | 0.1138         | 0.9250        | 1.1185   | 2  |  |
| R13        | 1.1000           | 0.8905        | 2.0807   | 0.1156         | 0.8048        | 1.3473   | 2  |  |
| R14        | 0.1810           | 0.5331        | 0.0000   | 0.3564         | 1.1059        | 0.0798   | 2  |  |
| R15        | 0.8299           | 0.5000        | 0.6609   | 0.1000         | 0.8331        | 0.5347   | 2  |  |
| R16        | 0.3426           | 0.5442        | 0.2217   | 0.1000         | 0.5000        | 1.2736   | 2  |  |
| <b>OBJ</b> | <b>14.2754 s</b> |               |          |                |               |          |    |  |

Table 7. Optimal settings of time-voltage-current-based dual-setting DOCRs in GCM using IEAM.

| Relay      | $TMS_{FW}$ (s)   | $PS_{FW}$ (A) | $\alpha$ | $TMS_{RV}$ (s) | $PS_{RV}$ (A) | $\alpha$ | CS |  |
|------------|------------------|---------------|----------|----------------|---------------|----------|----|--|
| R1         | 0.2475           | 0.9213        | 0.1788   | 0.3266         | 1.8058        | 1.5348   | 2  |  |
| R2         | 1.0906           | 0.9399        | 1.0931   | 0.1000         | 1.5000        | 1.0625   | 2  |  |
| R3         | 0.1000           | 1.5000        | 0.7509   | 0.9626         | 0.5801        | 1.6145   | 2  |  |
| R4         | 0.7273           | 0.8073        | 0.4231   | 0.1111         | 0.9664        | 0.8639   | 2  |  |
| R5         | 0.6325           | 1.1587        | 0.9600   | 0.4128         | 0.7335        | 1.6003   | 2  |  |
| R6         | 1.0941           | 0.5726        | 0.0156   | 0.3739         | 0.7881        | 0.6660   | 2  |  |
| R7         | 0.2253           | 0.5514        | 0.0352   | 0.9750         | 0.5642        | 0.6738   | 2  |  |
| R8         | 1.1000           | 0.5701        | 0.0156   | 0.2189         | 1.4729        | 2.3906   | 2  |  |
| R9         | 0.3795           | 0.9650        | 0.0811   | 0.6000         | 1.5000        | 3.2887   | 2  |  |
| R10        | 0.7939           | 0.8021        | 1.0987   | 0.6876         | 1.2294        | 1.1812   | 2  |  |
| R11        | 0.4673           | 1.3326        | 0.5636   | 0.2875         | 0.8865        | 0.6523   | 2  |  |
| R12        | 0.9750           | 0.7537        | 2.2972   | 0.5425         | 1.7083        | 1.1431   | 2  |  |
| R13        | 0.4374           | 1.0329        | 0.1094   | 0.9750         | 0.6178        | 1.1250   | 2  |  |
| R14        | 0.3878           | 0.6887        | 0.1550   | 0.9489         | 1.2590        | 1.5070   | 2  |  |
| R15        | 0.2485           | 0.5318        | 0.0156   | 0.4100         | 0.5000        | 1.4011   | 1  |  |
| R16        | 0.7600           | 0.7928        | 1.4233   | 0.8424         | 0.8203        | 1.5313   | 2  |  |
| <b>OBJ</b> | <b>11.1658 s</b> |               |          |                |               |          |    |  |

Table 8. Common optimal settings of time-voltage-current-based dual-setting DOCRs using IEAM.

| Relay      | $TMS_{FW}$ (s)   | $PS_{FW}$ (A) | $\alpha$ | $TMS_{RV}$ (s) | $PS_{RV}$ (A) | $\alpha$ | CS |
|------------|------------------|---------------|----------|----------------|---------------|----------|----|
| R1         | 0.9456           | 0.5000        | 0.3154   | 0.8188         | 0.9191        | 1.0996   | 2  |
| R2         | 0.5936           | 0.9063        | 0.3119   | 1.1000         | 0.5000        | 1.2188   | 2  |
| R3         | 0.1000           | 0.6916        | 1.0327   | 0.7689         | 0.5000        | 2.4856   | 3  |
| R4         | 0.9153           | 0.5000        | 1.5075   | 0.4690         | 0.8672        | 1.2761   | 1  |
| R5         | 0.1000           | 2.0000        | 0.6728   | 0.6929         | 0.5398        | 1.8929   | 1  |
| R6         | 0.7429           | 0.7046        | 0.0508   | 0.2058         | 1.4996        | 1.5185   | 2  |
| R7         | 0.1021           | 0.8114        | 0.6514   | 1.1000         | 0.5000        | 1.5703   | 1  |
| R8         | 0.1696           | 1.4361        | 0.0000   | 1.0684         | 0.8162        | 1.1333   | 2  |
| R9         | 0.6362           | 0.7808        | 0.1984   | 0.1453         | 1.8174        | 0.2454   | 2  |
| R10        | 0.6000           | 0.5000        | 1.3194   | 0.5103         | 1.4985        | 1.6390   | 1  |
| R11        | 0.7436           | 0.9619        | 0.3660   | 0.6002         | 0.5000        | 0.3843   | 2  |
| R12        | 1.1000           | 0.5000        | 1.5588   | 1.0844         | 1.3750        | 1.4314   | 2  |
| R13        | 0.7672           | 0.7609        | 0.0625   | 0.8500         | 0.5000        | 0.5242   | 2  |
| R14        | 0.1000           | 1.5000        | 0.4675   | 1.1000         | 0.7500        | 0.5708   | 2  |
| R15        | 0.2128           | 1.0057        | 0.6446   | 0.5438         | 0.6732        | 1.3003   | 1  |
| R16        | 0.1411           | 0.7574        | 0.5181   | 0.1849         | 1.4375        | 1.0186   | 1  |
| <b>OBJ</b> | <b>10.9450 s</b> |               |          |                |               |          |    |

Table 9. Coordination constraint violations in each operating mode.

| Settings calculated | Algorithm | Number of coordination constraint violations |     |                    |     |       |     |                    |     |
|---------------------|-----------|----------------------------------------------|-----|--------------------|-----|-------|-----|--------------------|-----|
|                     |           | GCM                                          |     |                    |     | ISM   |     |                    |     |
|                     |           | DOCRs                                        |     | Dual-setting DOCRs |     | DOCRs |     | Dual-setting DOCRs |     |
|                     |           | TC                                           | TCV | TC                 | TCV | TC    | TCV | TC                 | TCV |
| GCM                 | IEAM      | 0                                            | 0   | 0                  | 0   | 5     | 5   | 6                  | 6   |
| ISM                 | IEAM      | 11                                           | 11  | 12                 | 2   | 0     | 0   | 0                  | 0   |
| Common settings     | IEAM      | 0                                            | 0   | 0                  | 0   | 0     | 0   | 0                  | 0   |

\*TC: Time-current-based characteristic

\*TCV: Time-voltage-current-based characteristic

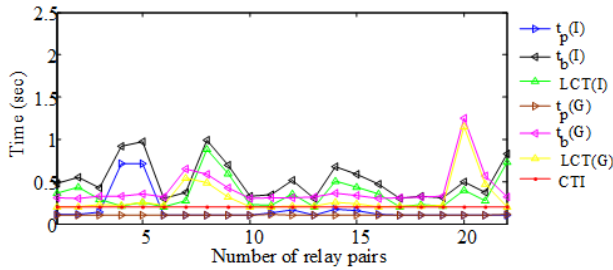


Fig. 8. Operating time and LCT of dual-setting relay pairs in GCM and ISM using IEAM.

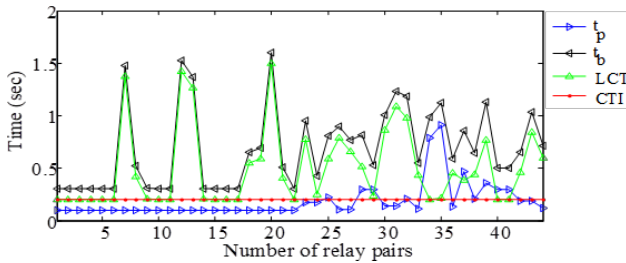


Fig. 9. Operating time and LCT of dual-setting relay pairs with common optimal settings using IEAM.

results are compared to the PSO and GA, which shows that IEAM performs better in terms of the total operating time of the DOCRs for both operating modes of the microgrid.

### 5. CONCLUSIONS

The performances of four coordination schemes, namely, conventional DOCRs, time-voltage-current-based DOCRs, dual-setting DOCRs, and proposed time-voltage-current based dual-setting DOCRs with MI characteristics, have been investigated to solve the relay coordination schemes. This paper proposes

a modified protection coordination scheme for microgrids with time-voltage-current-based dual-setting DOCRs. The proposed scheme considered MI characteristics to determine common optimal settings of time-voltage-current-based dual-setting DOCRs, providing proper coordination in both GCM and ISM. The protection coordination problem is formulated as an MINLP problem and optimally solved using IEAM. Based on the studies carried out in this paper, time-voltage-current-based dual-setting DOCRs has been found to be the best one among the four schemes studied. The proposed relay coordination scheme is shown to significantly reduce the operating time of relays compared to conventional approaches. On the other hand, it is found that with the common settings of DOCRs, proper coordination in both GCM and ISM can be achieved. Furthermore, it is found that the performance of IEAM is better compared to the PSO and GA concerning the total operating time of the relays. Future work can be extended to calculate the relay characteristics coefficient ( $A_D$  and  $B_D$ ) as continuous variables for estimating the performance of protection schemes with different standard and user-defined relay characteristics.

### DECLARATIONS

**Conflict of interest** The authors declare no conflicts of interest regarding this article.

**Research involving Human Participants and/or Animals** This article contains no studies with human participants or animals performed by authors.

**Informed consent** All authors have approved the manuscript and agree with its submission to the Journal for publication.

### REFERENCES

[1] A. C. Adewole, A. D. Rajapakse, D. Ouellette, and P. Forsyth, "Protection of active distribution networks incorporating microgrids with multi-technology distributed energy resources," *Electr. Power Syst. Res.*, vol. 202, p. 107575, 2022.



Table 10. Comparative analysis of the total operating time of DOCRs using standard and time-voltage-current-based characteristics.

| Mode           | Algorithm | Total operating time (second) |       |                    |       | % Percentage reduction in time compared with time-voltage-current-based dual-setting DOCRs |       |                    |
|----------------|-----------|-------------------------------|-------|--------------------|-------|--------------------------------------------------------------------------------------------|-------|--------------------|
|                |           | DOCRs                         |       | Dual-setting DOCRs |       | DOCRs                                                                                      |       | Dual-setting DOCRs |
|                |           | TC                            | TCV   | TC                 | TCV   | TC                                                                                         | TCV   | TC                 |
| GCM            | IEAM      | 21.05                         | 20.88 | 16.75              | 14.27 | 32.20                                                                                      | 31.65 | 14.80              |
|                | PSO       | 25.52                         | 23.46 | 18.73              | 17.58 | 31.31                                                                                      | 25.06 | 6.13               |
|                | GA        | 26.33                         | 24.34 | 19.45              | 18.50 | 29.73                                                                                      | 23.99 | 4.88               |
| ISM            | IEAM      | 21.96                         | 21.05 | 18.47              | 11.16 | 49.18                                                                                      | 46.98 | 39.57              |
|                | PSO       | 29.21                         | 28.21 | 22.32              | 14.67 | 49.77                                                                                      | 47.99 | 34.27              |
|                | GA        | 30.11                         | 28.90 | 23.67              | 15.02 | 50.11                                                                                      | 48.02 | 36.54              |
| For both modes | IEAM      | 15.13                         | 13.79 | 11.45              | 10.94 | 27.69                                                                                      | 20.66 | 10.40              |
|                | PSO       | 17.98                         | 16.85 | 15.29              | 13.76 | 23.47                                                                                      | 18.33 | 10.00              |
|                | GA        | 18.45                         | 17.21 | 16.98              | 15.01 | 18.64                                                                                      | 12.78 | 11.60              |

- [2] D. A. Gadanayak, "Protection algorithms of microgrids with inverter interfaced distributed generation units—a review," *Electr. Power Syst. Res.*, vol. 192, p. 106986, 2021.
- [3] H. A. Alsiraji and J. M. Guerrero, "A new hybrid virtual synchronous machine control structure combined with voltage source converters in islanded ac microgrids," *Electr. Power Syst. Res.*, vol. 193, p. 106976, 2021.
- [4] A. Chandra, G. K. Singh, and V. Pant, "Protection of ac microgrid integrated with renewable energy sources—a research review and future trends," *Electr. Power Syst. Res.*, vol. 193, p. 107036, 2021.
- [5] M. Faghihi Rezaei, M. Gandomkar, and J. Nikoukar, "Optimizing multi-objective function for user-defined characteristics relays and size of fault current limiters in radial networks with renewable energy sources," *J. Oper. Autom. Power Eng.*, vol. 12, no. 1, pp. 42–53, 2024.
- [6] M. N. Alam, "Overcurrent protection of ac microgrids using mixed characteristic curves of relays," *Comput. Electr. Eng.*, vol. 74, pp. 74–88, 2019.
- [7] A. Darabi, M. Bagheri, and G. B. Gharehpetian, "Highly sensitive microgrid protection using overcurrent relays with a novel relay characteristic," *IET Renewable Power Gener.*, vol. 14, no. 7, pp. 1201–1209, 2020.
- [8] A. Yazdanejadi, M. S. Naderi, G. B. Gharehpetian, and V. Talavat, "Protection coordination of directional overcurrent relays: new time current characteristic and objective function," *IET Gener. Transm. Distrib.*, vol. 12, no. 1, pp. 190–199, 2018.
- [9] P. Niranjana, R. K. Singh, and N. K. Choudhary, "Comparative study of relay coordination in a microgrid with the determination of common optimal settings based on different objective functions," *Int. J. Eng. Tech. Innovation*, vol. 12, no. 3, pp. 260–273, 2022.
- [10] H. Shad, M. Gandomkar, and J. Nikoukar, "An improved optimal protection coordination for directional overcurrent relays in meshed distribution networks with dg using a novel truth table," *J. Oper. Autom. Power Eng.*, vol. 11, no. 3, pp. 151–161, 2023.
- [11] R. Tiwari, R. K. Singh, and N. K. Choudhary, "Coordination of dual setting overcurrent relays in microgrid with optimally determined relay characteristics for dual operating modes," *Prot. Control Mod. Power Syst.*, vol. 7, no. 1, pp. 6–24, 2022.
- [12] A. A. Balyith, H. M. Sharaf, M. Shaaban, E. F. El-Saadany, and H. H. Zeineldin, "Non-communication based time-current-voltage dual setting directional overcurrent protection for radial distribution systems with dg," *IEEE Access*, vol. 8, pp. 190572–190581, 2020.
- [13] A. Hatata, A. Ebeid, and M. El-Saadawi, "Optimal restoration of directional overcurrent protection coordination for meshed distribution system integrated with dgs based on fcls and adaptive relays," *Electr. Power Syst. Res.*, vol. 205, p. 107738, 2022.
- [14] M. N. Alam, "Adaptive protection coordination scheme using numerical directional overcurrent relays," *IEEE Trans. Ind. Inf.*, vol. 15, no. 1, pp. 64–73, 2018.
- [15] T. Khurshaid, A. Wadood, S. G. Farkoush, C.-H. Kim, J. Yu, and S.-B. Rhee, "Improved firefly algorithm for the optimal coordination of directional overcurrent relays," *IEEE Access*, vol. 7, pp. 78503–78514, 2019.
- [16] D. Sarkar and S. Kudkelwar, "Optimal over current relay coordination in microgrid using a novel hybrid water cycle-moth flame algorithm," *Int. J. Syst. Assur. Eng. Manage.*, vol. 12, no. 3, pp. 553–564, 2021.
- [17] Y. Damchi, J. Sadeh, and H. R. Mashhadi, "Applying hybrid interval linear programming and genetic algorithm to coordinate distance and directional over-current relays," *Electr. Power Compon. Syst.*, vol. 44, no. 17, pp. 1935–1946, 2016.
- [18] P. Omid, S. Abazari, and S. Madani, "Optimal coordination of directional overcurrent relays for microgrids using hybrid interval linear programming-differential evolution," *J. Oper. Autom. Power Eng.*, vol. 10, no. 2, pp. 122–133, 2022.
- [19] A. Tjahjono, D. O. Anggriawan, A. K. Faizin, A. Priyadi, M. Pujiantara, T. Taufik, and M. H. Purnomo, "Adaptive modified firefly algorithm for optimal coordination of overcurrent relays," *IET Gener. Transm. Distrib.*, vol. 11, no. 10, pp. 2575–2585, 2017.
- [20] A. Chawla, B. R. Bhalja, B. K. Panigrahi, and M. Singh, "Gravitational search based algorithm for optimal coordination of directional overcurrent relays using user defined characteristic," *Electr. Power Compon. Syst.*, vol. 46, no. 1, pp. 43–55, 2018.
- [21] D. Saha, A. Datta, and P. Das, "Optimal coordination of directional overcurrent relays in power systems using symbiotic organism search optimisation technique," *IET Gener. Transm. Distrib.*, vol. 10, no. 11, pp. 2681–2688, 2016.
- [22] M. Ghotbi Maleki, R. Mohammadi Chabanloo, and H. Javadi, "Method to resolve false trip of non-directional overcurrent relays in radial networks equipped with distributed generators," *IET Gener. Transm. Distrib.*, vol. 13, no. 4, pp. 485–494, 2019.
- [23] D. S. Alkaran, M. Vatani, M. J. Sanjari, G. B. Gharehpetian, and M. S. Naderi, "Optimal overcurrent relay coordination in interconnected networks by using fuzzy-based ga method," *IEEE Trans. Smart Grid*, vol. 9, no. 4, pp. 3091–3101, 2016.
- [24] H. R. Baghaee, M. Mirsalim, G. B. Gharehpetian, and H. A. Talebi, "Mopso/fdmt-based pareto-optimal solution for

- coordination of overcurrent relays in interconnected networks and multi-der microgrids," *IET Gener. Transm. Distrib.*, vol. 12, no. 12, pp. 2871–2886, 2018.
- [25] K. Mishra, S. Tiwari, and A. Misra, "A bio inspired algorithm for solving optimization problems," in *2011 2nd Int. Conf. Comput. Commun. Technol. (ICCCCT-2011)*, pp. 653–659, IEEE, 2011.
- [26] K. Mishra, S. Tiwari, and A. K. Misra, "Improved environmental adaption method for solving optimization problems," in *Int. Symp. Intell. Comput. Appl.*, pp. 300–313, Springer, 2012.
- [27] R. D. Christie, "'power systems test case archive", available at: <https://labs.ece.uw.edu/pstca/pf14/pgtca14bus.htm>," 1999.